Received: 11 November 2019 | Revised: 15 January 2020 | Accepted: 15 January 2020

DOI: 10.1002/mmce.22178

RESEARCH ARTICLE

INTERNATIONAL JOURNAL OF RF AND MICROWAVE COMPUTER-AIDED ENGINEERING WILEY

Beam scanning annular slot-ring antenna array with via-fence for wireless power transfer

Laxmikant Minz | **Seong-Ook Park**

Department of Electrical Engineering, Korea Advanced Institute of Science and Technology, Daejeon, South Korea

Correspondence
Laxmikant Minz, Department of Electrical Engineering
Korea Advanced Institute of Science and Technology, Daejeon, South Korea.
Email: lkminz@kaist.ac.kr

Funding information
National Research Foundation of Korea (NRF), Grant/Award Number: 2019R1A2B5B01069407

Abstract

Wireless power transfer has been the field of research for many decades, and with technological advancement and increase in wireless mobile devices, the future of wireless power transfer technology is very promising. The major requirement of wireless power transfer is an efficient and compact antenna array with high gain and flawless scanning performance. In this article, a 4×8 element array is proposed with a gain of 18 dB and scanning capability of $\pm 45^{\circ}$ in azimuth and elevation plane at 5.8 GHz. The overall size of the array is 100 mm $\times$ 200 mm. The element separation in the array is only 0.48 λ. There was strong mutual coupling due to smaller separation, which has been minimized with the application of via-fence around the antenna element. A dual feed circularly polarized annular slot-ring antenna is proposed and analyzed with via-fence to develop an array of 4×8 elements. The antenna array reflection coefficient obtained is less than 20 dB for different scan angles and the gain of the array obtained is also within 2 dB for $\pm 45^{\circ}$ scan angles.

KEYWORDS

annular slot-ring, beam scanning, mutual coupling, MWPT, stripline feeding, via-fence

1 | INTRODUCTION

Microwave wireless power transfer (MWPT) is a perennial technology, initially demonstrated by Tesla in 1891 and since then there has been an extensive research in this domain. For mobile devices like smartphones, the best accomplishment engineered so far is inductive charging. Wireless inductive chargers are commercially available, where wire tethering is gone but the device is still required to be in close bound to the charging pad for its charging. Research on long-range wireless power transfer[1] is progressing and currently focusing on installation of multiple charging panels with a controlling base station for charging multiple mobile/portable electronics devices over a range of 5 to 20 m, Figure 1. Applications of MWPT are extending to RFIDs, IoTs, and even to power lines.[2] Among the various challenges from DC-to-RF power conversion efficiency to beam focusing and multidevice charging, an efficient transmitter antenna array design is a prime component for the overall MWPT system.

In this article, we present a circularly polarized (CP), efficient, and compact wide-angle beam-steering 4×8 antenna array design for long-range MWPT system. There are different challenges in design of a beam-steering antenna array for MWPT. First is the mutual coupling, which affects impedance matching, reflection coefficient, radiation pattern, gain, steering angle with relative phase shift, and so on. The coupling between elements varies the antenna characteristics and prohibits compactness. Various research works have been conducted to study the mutual coupling effect in an array and various techniques have been proposed to reduce the mutual coupling.[3-5] Parasitic patches and parasitic

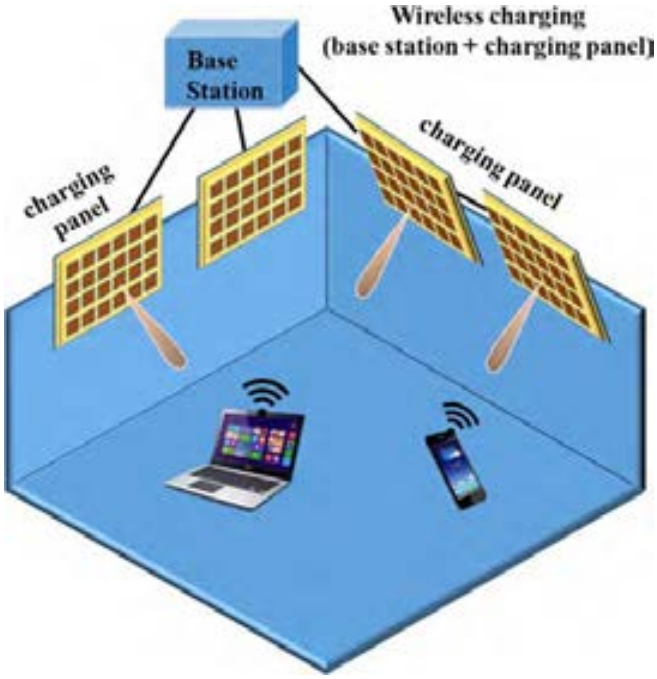

FIGURE 1 Long-range multipanel wireless charging scheme

meander line,[6,7] soft or hard surfaces, defected ground structure,[8] bandgap structure,[9-11] metamaterial,[12] and electromagnetic three-dimensional (3D) wall[13] are a few techniques proposed in the literature to reduce mutual coupling by blocking or minimizing surface current flow. These techniques are in common practice and easier to fabricate (if planar); however, they are complex to comprehend and design. In addition, they often consume more time than antenna element design. Here we proposed a via-fence structure to minimize mutual coupling between antenna elements. The proposed via-fence is a simple structure with multiple vias of diameter and separation as small as possible as per fabrication limitation, described in subsequent sections. Similar decoupling cavity structures, made up of metal ring boundary shorted with vias, were found to be simple in fabrication and effective to reduce mutual coupling.[14-17] Antennas with via loading have been used in earlier research for gain and bandwidth enhancement;[18,19] we applied them here for mutual coupling reduction and to improve closely spaced antenna array performance.

Second, the critical factor of an array panel employed for MWPT system is its beam-steering capability. The beam-steering ability of the array is required to be a maximum of $\pm 45^{\circ}$ because a $\pm 45^{\circ}$ steering would be sufficient to direct the high gain beam toward a device in any location over the confined space as in Figure 1. A wide-angle beam-steering antenna array can be obtained either with wide-beam antenna or with wide-angle impedance matching.[20] Recent work on antenna array for MWPT[21-23] has steering capability of $\pm 30^{\circ}$, $\pm 39^{\circ}$, and $\pm 40^{\circ}$, respectively. Beam-steering capability depends on antenna element size and array element separation. A small element size annular slot-ring antenna is opted for the antenna array design as it has smaller size compared to conventional rectangular patch antennas and disk patch antenna. Moreover, due to simple construction slot-ring microstrip antenna can be easily integrated with RF components of the MWPT system. There is a size constraint of 25 mm × 25 mm ($0.48\,\lambda \times 0.48\,\lambda$) for single element due to the MPWT system in hand and the designed slot-ring antenna adjusted well in the limited area.

Lastly, efficiency of the antenna is important for MWPT system. Low reflection coefficient and low dielectric loss are essential for radiation efficiency, whereas low polarization mismatch and high gain can minimize path loss and improve power transmission efficiency. Polarization mismatch can be avoided with circular polarized antenna array. The designed annular slot-ring antenna is CPusing dual feed offset with 90° phase shift. The annular slot-ring antenna is fed through proximity coupling. The advantage of using proximity-coupled feed is that it inherently blocks harmonics. The harmonic signal generated by rectifying circuit could interfere with other signals and reduce the rectenna efficiency in MWPT system.

The designed CP annular slot-ring microstrip antenna element operates at 5.8 GHz. The gain of the 4 × 8 array (200 mm × 100 mm) obtained is as high as 18 dB. In this article, the annular slot-ring antenna design and performance is described in Section 2. Mutual coupling in slot-ring antenna and effect of coupling while forming array is presented in Section 3. The proposed annular slot-ring antenna with via-fence characteristics and results are presented in Section 4. A single and double via-fence analysis is presented in Section 5. Then the 4 × 8 array model of annular slot-ring design with via fence using unit cell approach is presented with fabricated array result in Section 6.

2 | ANNULAR SLOT-RING ANTENNA

An annular slot-ring microstrip antenna has various benefits. First, a slot-ring antenna is smaller and has an easy construction than other planar or nonplanar antennas.[24,25] In terms of construction, the slot-ring size is apparently not affected by the dielectric permittivity, which is a unique phenomenon compared with microstrip patch antenna, where structure fields diffuse through both substrate and free space, and the dielectric constant directly affect the patch dimension. The size of the slot entirely depends on fundamental operating

frequency. The fundamental operating frequency of the slot-ring is the frequency for which mean circumference of the slot-ring is equal to wavelength (λ). It can be formulated as[26]:

$$kr_a = 1 \tag{1}$$

where $k = \frac{2\pi}{\lambda}$ is the wave number and r_a is the average of outer and inner radius of slot-ring. A stripline feed slot-ring antenna is shown in Figure 2. Top layer consists of a metallic layer with a slot-ring on it. The slot-ring is feed through proximity coupling using a stripline feed, shown in shades. The symmetric structure of the ring makes it easier to get circular polarization. In Figure 2, two stripline feeds are utilized to obtain a circular polarized or a dual linear polarized antenna by mere control of phase between two feeds. These striplines are feed through coaxial cable from the bottom. A circular pad is utilized at the end of the stripline to assist the transition from coax to stripline.

The slot-ring antenna shown in Figure 2 is designed to operate at 5.8 GHz. For 5.8 GHz, the optimized slot-ring dimensions are as follows: a = 7.7 mm, ws = 0.83 mm, and fle = 4.28 mm. A thin and low permittivity substrate of permittivity, ϵr = 3.0 and thickness, h = 0.76 mm is utilized. The overall length and width of the substrate are fixed to be 25 mm and 25 mm, respectively, as per the constraint. The designed annular slot-ring antenna is simulated using commercial software (CST MWS), and the simulated s-parameter results are shown in Figure 3.

The simulated results in Figure 3 show that both S_{11} and S_{22} have good matching at 5.8 GHz and the S_{21} (or S_{12}) is below 20 dB, indicating that two ports are isolated enough to operate antenna for dual linear polarization as well as circular polarization if the phase difference between two ports is 90°. The circular polarized matching performance is also shown in Figure 3 by a plot with label S_{11} [1, 0] + S_{22} [1, 90], highlighting that signals at port 1 and port 2 are of the same amplitude and the port 2 phase is shifted by 90°. The radiation pattern of the designed slot-ring antenna for linear polarization (port 1 or port 2) and circular polarization is shown in Figure 4. The gain of slot-ring is 6.9 dB.

The single-element characteristics, such as high gain, good matching, and small size, obtained through simulation are suitable for compact MPWT system. Other characteristics of the antenna required to examine for MWPT system is the beam scanning of the array developed from the designed single antenna element. In an array development, two important aspects are required to be considered: (a) element spacing to avoid grating lobes while scanning and (b) mutual coupling, which would affect the input impedance matching and radiation characteristics of the overall antenna. The maximum beam scanning possible from the designed element without grating lobes can be estimated through beam scanning capacity equation as follows[27]:

$$d_{\max} = \frac{\lambda}{1 + sin\theta} \tag{2}$$

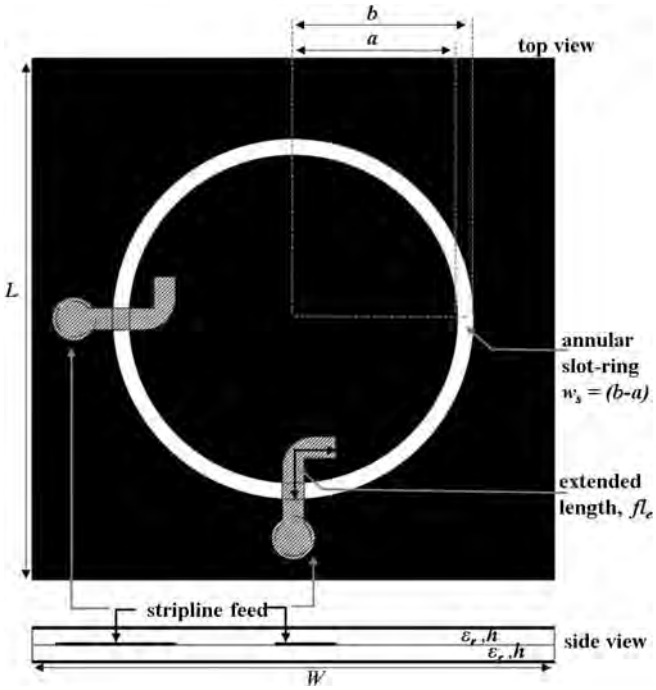

FIGURE 2 Annular slot-ring antenna model with top and side views

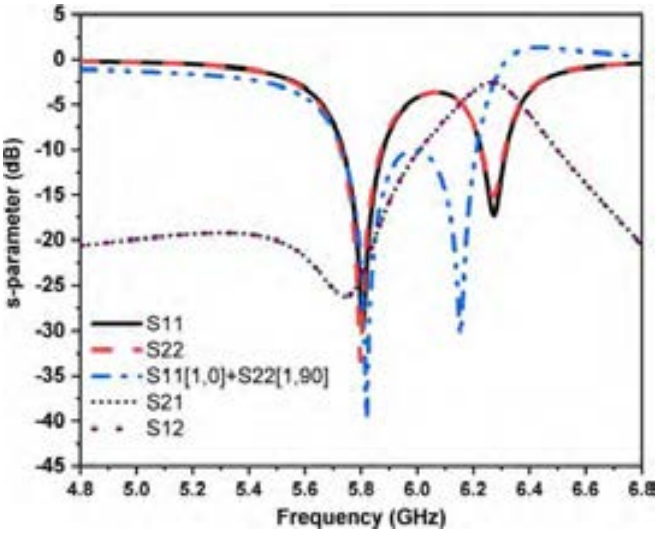

FIGURE 3 S-parameter plot of annular slot-ring

where d_{max} is the maximum distance between the antenna element, θ is the scan angle, and the λ is the wavelength. From Equation (2), it can be calculated that for beam scanning of $\pm 45^{\circ}$, d_{max} should be less than 0.54 λ. The designed element size is 0.48 $\lambda \times$ 0.48 λ; therefore, it is suitable for beam scanning requirement of the MWPT array panel in both elevation and azimuth plane. The beam-steering performance of the array from single-element characteristics could be achieved, for verification, without actual simulation with the product of single-element pattern by planar array factor (AF) expression. A normalized form of planar AF for M×N element array is given by[28]:

$$AF = \left[\sum_{m=1}^{M} e^{j(m-1)(kd_x sin\theta cos\phi + \beta_x)}\right] \left[\sum_{n=1}^{N} e^{j(n-1)\left(kd_y sin\theta sin\phi + \beta_y\right)}\right] \quad (3)$$

where k is wave number, M is number of elements placed at d_x distance separation with β_x progressive phase shift between them, and N is number of elements placed at d_y distance separation with β_y progressive phase shift between them. The MWPT system for which the antenna array is designed (Figure 1) a $\pm$ 45° in azimuth plane and elevation plane would be sufficient, therefore the scanning performance of 4×8 slot-ring array for ±45° in azimuth and $\pm$ 45° in elevation plane is calculated from Equation (3) and shown in Figure 5. There are no grating lobes in the scanning range and the gain of the pattern for different scan angles is within 3 dB range. The number of element in azimuth plane is eight and in elevation plane is four, therefore beam width of radiation pattern in azimuth plane is narrow than elevation plane.

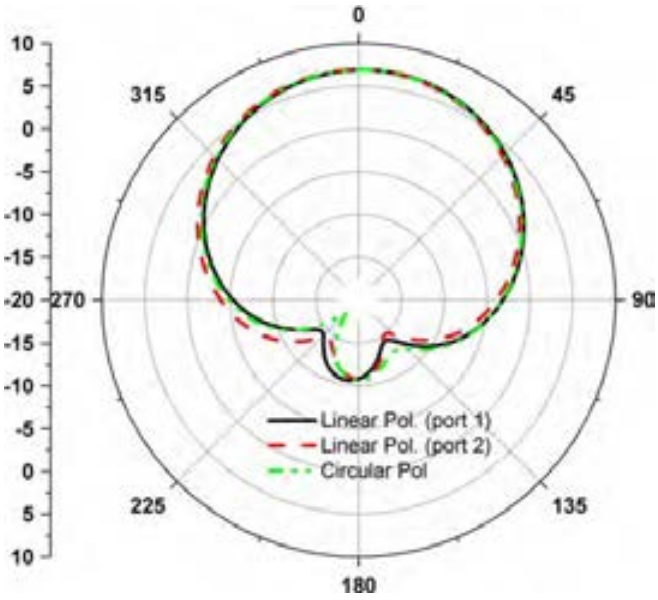

FIGURE 4 Radiation pattern of the slot-ring

3 | MUTUAL COPULING IN ANNULAR SLOT-RING ANTENNA

Analytical results obtained from Equation (3) shows a beam-steering capability of the slot-ring antenna owing to its size and element separation. Mutual coupling is not

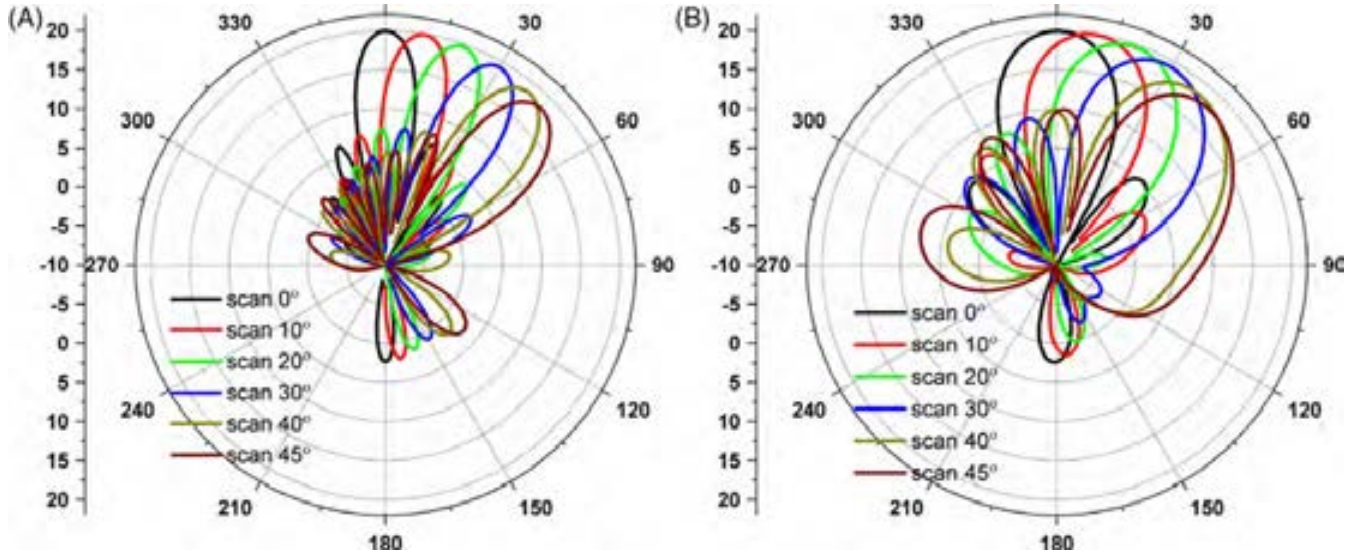

FIGURE 5 4 × 8 array beam scanning in A, azimuth plane and B, elevation plane

considered in this result. However, in a phased array antenna, the electromagnetic characteristics of an antenna element influence the other elements in its vicinity and the antenna element itself gets influenced due to other elements in proximity. Due to coupling the antenna array terminal impedance changes, matching performance get affected and the gain decreases. The mutual coupling effect on the slot-ring antenna can be studied by an array of two slot-ring model, as shown in Figure 6. A comparative reflection coefficient of the single-element and two-element array in Figure 7 shows that the mutual coupling affects the terminal impedance and deteriorates the matching performance at desire frequency of 5.8 GHz. Moreover, a comparative radiation pattern plot of two-element array and an analytical two-element radiation pattern obtained from product of single-element radiation pattern and AF is shown in Equation (3). Figure 8 shows that there is slight reduction in gain and the beam width became too wide with high back lobe due to mutual coupling effect. In Figure 9, E-field distribution spread over two elements when both antenna elements are excited simultaneously, which showcase the influence of the surface wave and the extent of mutual coupling between two elements.

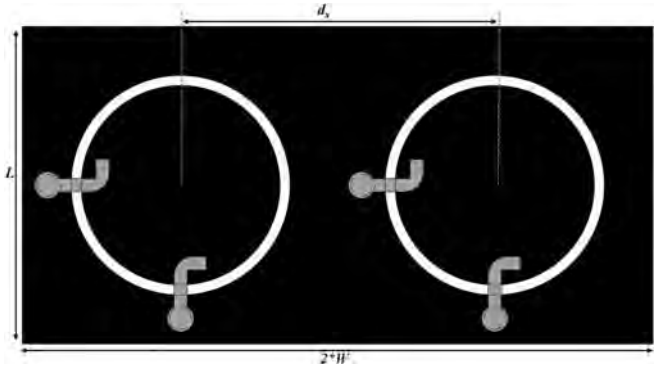

FIGURE 6 Two-element array of annular slot-ring antenna model with separation of d_x

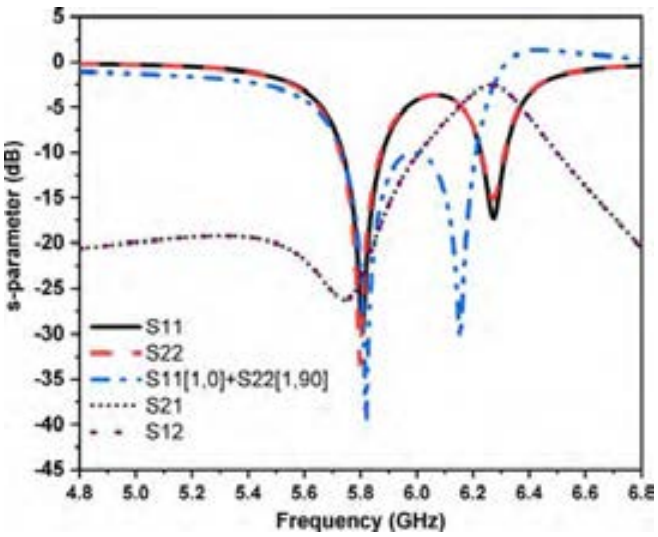

FIGURE 7 Comparison of terminal impedance matching of one-element and two-element array of slot-ring

4 | ANNULAR SLOT-RING ANTENNA WITH VIA-FENCE

With increase in number of elements, the mutual coupling effect would be worse and it is necessary to take measures in order to reduce the mutual coupling. Surface

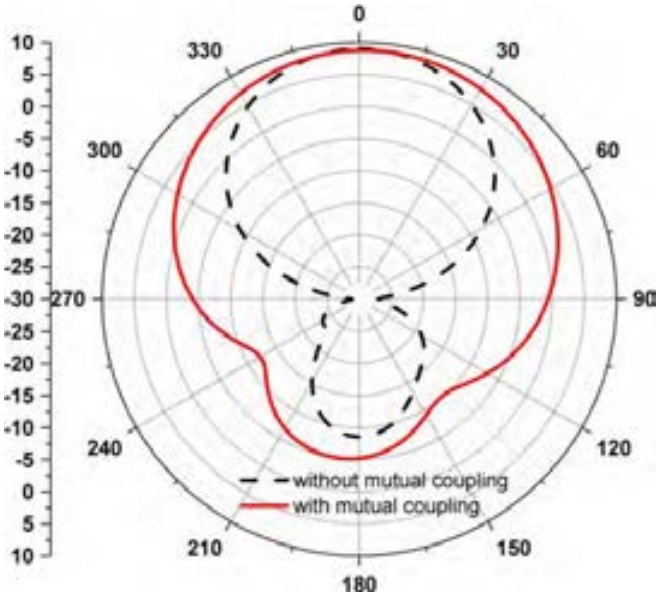

FIGURE 8 Comparison of radiation pattern of two-element array with and without mutual coupling

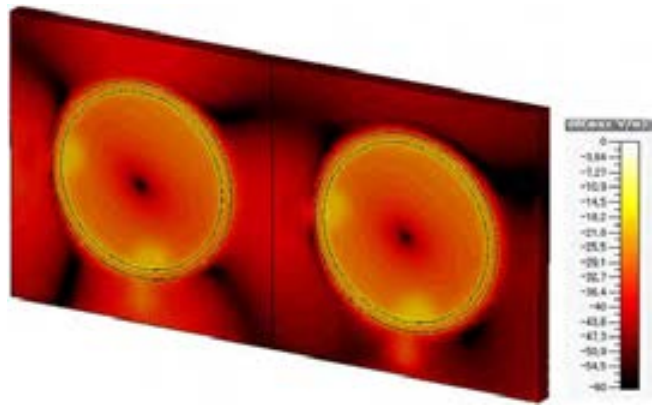

FIGURE 9 E-field distribution on the top layer of two slot-ring array when both antenna elements are simultaneously excited

current is the main factor for the coupling between the neighboring antenna elements.[24] A low permittivity and a thin substrate is preferred to alleviate surface current but additional technique is required to control it further.

We proposed a simple and easy to fabricate annular slot-ring structure with metal via-fence around it to suppress surface wave and reduce mutual coupling. The proposed design is shown in Figure 10. There are metal vias surrounding the dual feed slot-ring at regular interval of separation, V_s, and the via diameter is V_d. A via-fence has been utilized earlier for different applications. Substrate-integrated waveguide [29] and substrate-integrated coaxial line (SICL)[30] are the two popular form of via fencing application in microwave field as novel planar transmission lines. Via fencing around PCB circuits and microstrip lines has substantiated its effectiveness in reducing crosstalk[31,32] and its common guideline to use via-fence around PCB circuits for better performance. The present proposed model is motivated from such application of via-fence and applied here around a slot-ring antenna to be able to contain the signals and waves within the boundary of unit element and not let it interfere with and get affected from the other elements in proximity.

The proposed structure consist of a dual feed annular slot-ring antenna as in Figure 2 with the same parameter, slightly optimized to operate at 5.8 GHz, designed over same low permittivity substrate, Taconic RF 30 ($\epsilon_r = 3$, h = 0.76 mm). The effect of via-fence around the slot-ring is observed and verified by two-element array simulation. Similar to Figure 6, two proposed dual feed slot-ring antenna, separated by distance d_x (= 25 mm), with via-fence around each element is simulated with all the feed ports excited simultaneously, Figure 11. Figure 12 shows the E-field distribution over two-antenna element. From Figure 12, it can be observed that high magnitude of E-field is contained within the single antenna boundary and very low magnitude, <50 dB is only spreading over the two-antenna element. Comparing Figure 12 with Figure 9, we observe that with via-fence around the slot-ring E-field propagation from one element to another has been reduced by 20 to 25 dB. The metal via-fence blocks the surface current and isolates the elements in an array environment. The effect of isolation can be reflected from an unperturbed terminal impedance and radiation characteristics of antenna array. A two slot-ring antenna model with via-fence reflection coefficient characteristics and radiation pattern is shown in Figure 13 and Figure 14. Figure 13 shows that the reflection coefficient plots of slot-ring antenna for single element with via-fence and the reflection coefficient plot of two elements

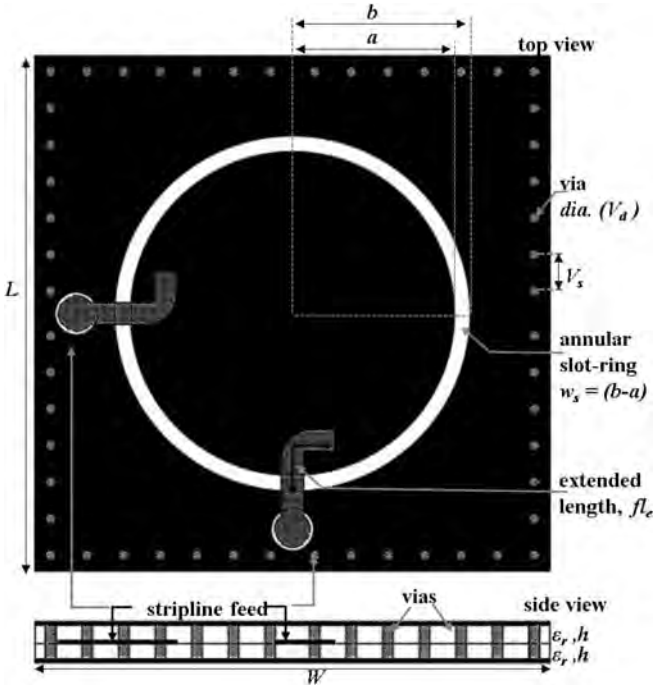

FIGURE 10 Annular slot-ring antenna model with via-fence

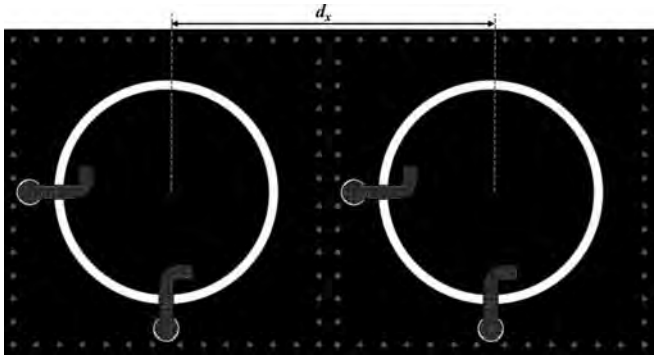

FIGURE 11 Two-element array of annular slot-ring antenna model with via-fence

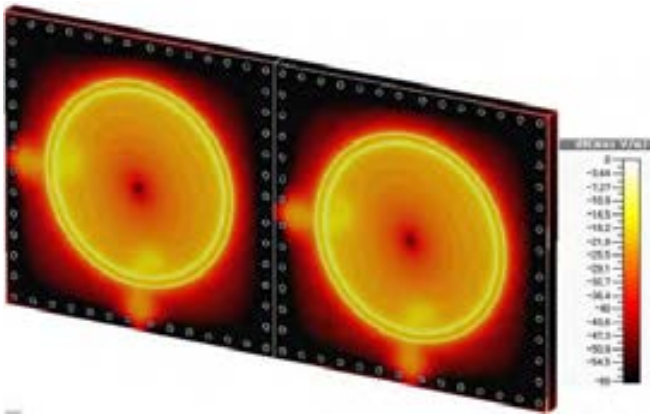

FIGURE 12 E-field distribution on the top layer of two proposed unit element arrays when both antenna elements are simultaneously excited

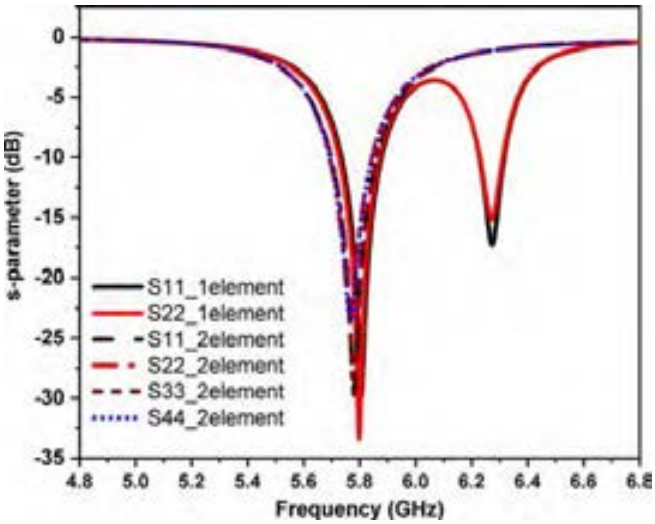

FIGURE 13 Comparison of terminal impedance matching of one-element and two-element array of slot-ring with via-fence

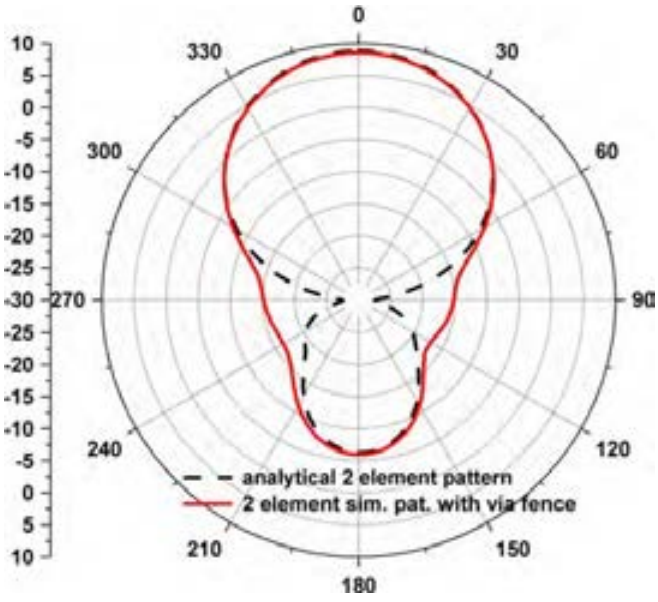

FIGURE 14 Comparison of analytical and simulated radiation pattern of two-element array of slot-ring with via-fence

array of slot-ring antenna with via-fence are similar. Therefore, compared with Figure 7, the mutual coupling effect causing deterioration of antenna matching has been diminished by use of via-fence around slot-ring antenna. Likewise, comparing Figure 13 with Figure 8, due to mitigated mutual coupling effect, the gain of two-element array as well as pattern of the array is similar to the analytically obtained two-element array result with no mutual coupling. The improvement in mutual coupling by measuring the transmission coefficient (isolation) between the two elements with and without via fence is shown in Figure 15. A comparison of isolation

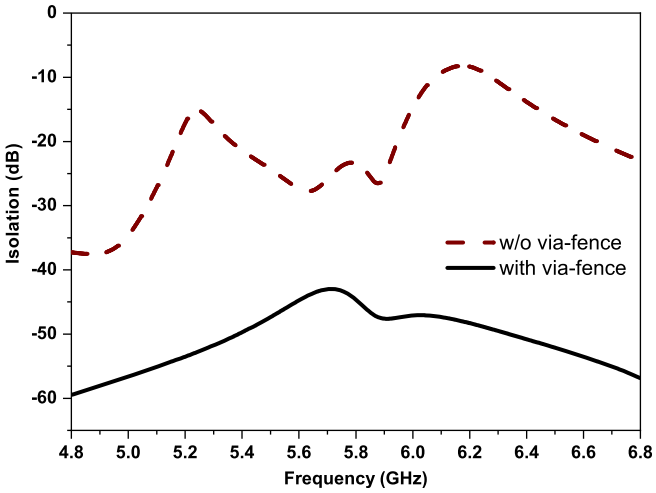

FIGURE 15 Isolation between two antenna elements with and without via-fence

TABLE 1 Mutual coupling reduction comparison

	Technique	Edge separation (λ_o)	Isolation improvement (dB)
This work	Via-fence	0.15	23
13	Three-dimensional wall	0.13	29
33	Parasitic meander line	0.6	6–10
34	Parasitic line	0.07	26
35	EBG and SRR	0.19	41
36	Metasurface	13.3	11.18
37	Polarization isolator	0.39	22.3

improvement of the current work with other recent works is presented in Table 1.

The advantage of the proposed structure is that the vias are connected at the boundary of the substrate within the limited space available after slot-ring and stripline feed design. There is no additional space requirement to apply vias. The overall structure is simple and can be easily fabricated. The design of via-fence is easy to comprehend and apply. A detailed analysis of via-fence is presented in the next section. The use of vias has not affected the simple construction of slot-ring antenna.

5 | VIA-FENCE ANALYSIS

The results of annular slot-ring antenna with via-fence is remarkable. This prompts for some experimentation with

via-fence parameters for its analysis. A via-fence is design with two parameters V_s and V_d. In order to analyze the via-fence, a model with via-fence at the center of a substrate (Taconic RF-30, $\epsilon_r = 3$, h = 0.76 mm) is designed, as shown in Figure 16, and wave ports are applied at the two ends of substrate. We intended to investigate the via-fence ability to obstruct the signal transmission from port 1 to port 2, and its behavior over frequency. Figure 17 shows the parametric study of via separation variation over frequency range of 0.1 to 40 GHz. Our frequency of interest is 5.8 GHz. We can observe that with smaller via separation, the transmission from port 1 to port 2, S_{21} decreases at 5.8 GHz. In other investigations, we observe the via-fence transmission characteristics with variation in V_d only by keeping the V_s constant. Figure 18 shows S_{21} for $V_s = 1.57$ mm at various values of V_d. There is a decrease in S_{21} with an increase in V_d. Examining Figure 17 and Figure 18, it can be asserted that more closer the vias, with smaller V_s and bigger V_d, more better the blocking of the passing signal at 5.8 GHz.

Intuitively, more number of via-fence could have better blocking performance. Our approach is to keep the size of antenna element small and apply the via-fence within the size constraint; therefore, we applied one row of via-fence around the designed slot-ring (Figure 10); however, apparently in our array design (Figure 11), single via-fence around antenna leads to two via-fences between slot-ring antenna elements. Two via-fences with a gap of V_{gap} between them are also analyzed in a similar way to single via-fence. Figure 19 shows a two-via-fence analysis model. The parametric study of two via-fences with variable V_s is presented in Figure 20. The S_{21} value at 5.8 GHz is lower for two fences than for a single fence. The parametric study of via diameter, V_d, keeping V_s

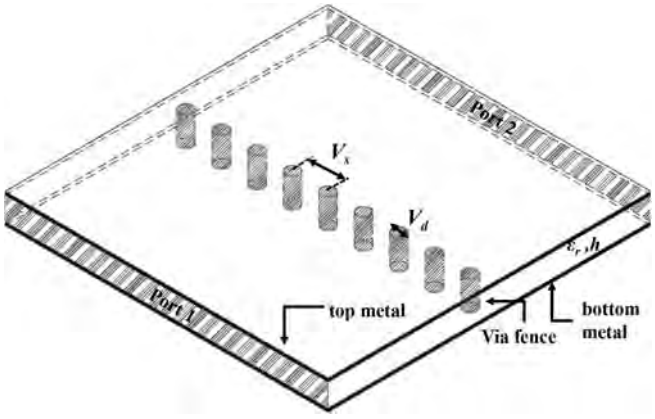

FIGURE 16 Single via-fence analysis model

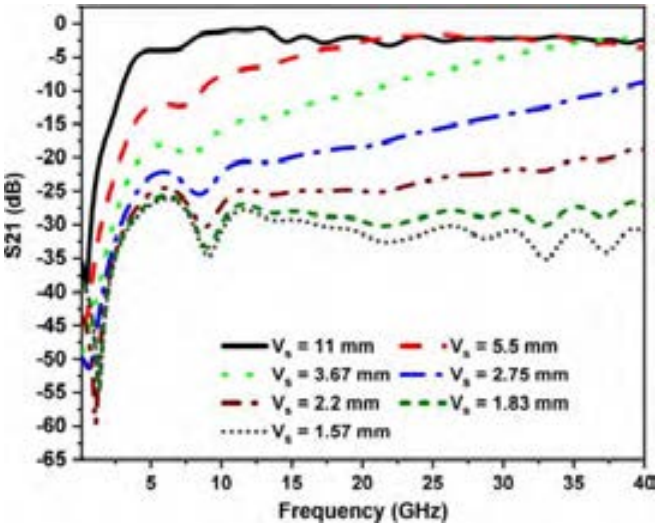

FIGURE 17 Transmission characteristics of single fence with variable V_s for $V_d = 1$ mm

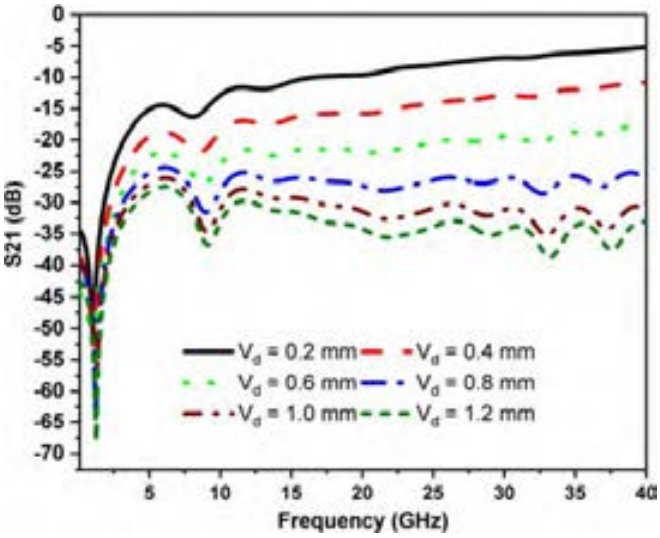

FIGURE 18 Transmission characteristics of single fence with variable V_d at $V_s = 1.57$ mm

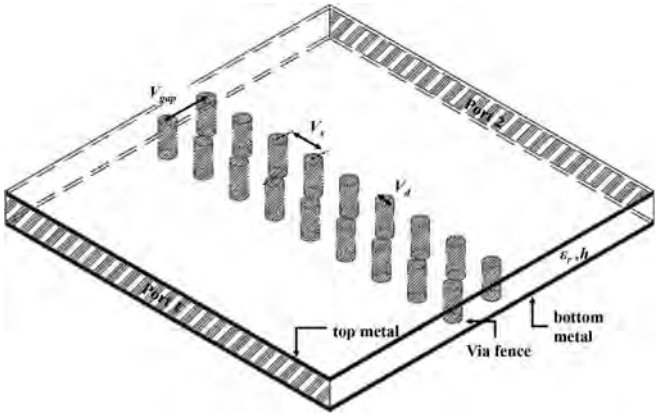

FIGURE 19 Two via-fence analysis model

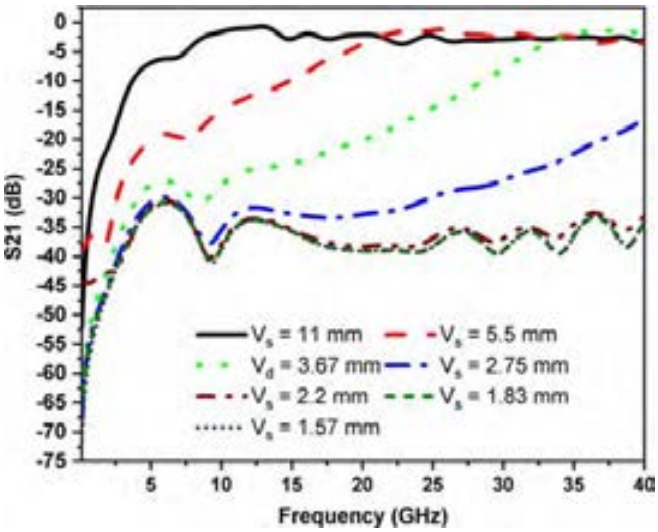

FIGURE 20 Transmission characteristics of two fence with variable V_s at $V_d = 0.5$ mm

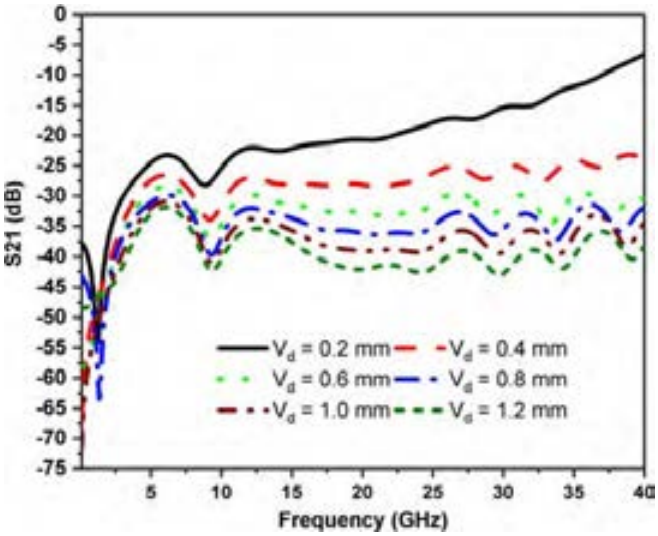

FIGURE 21 Transmission characteristics of two fence with variable V_d at $V_s = 1.57$ mm

fixed at 1.57 mm is shown in Figure 21. The variation of transmission signal is similar to the single-fence analysis, but isolation of port 1 and port 2 is better in two via-fences. S_{21} values at 5.8 GHz for various V_s and V_d values in terms of λ are tabulated in Table 2 and Table 3, respectively, for better insight.

It can also be observed that signal blockage deteriorates with the increase in frequency. Such characteristics can be relatable to a high-pass filter. For $V_s = 11$ mm and $V_s = 5.5$ mm in a single fence, a clear transition of signal from stop-band to pass-band is visible. Considering the range from maximum S_{21} value to 3 dB below maximum value as pass-band then cutoff frequency for $V_s = 11$ mm,

TABLE 2 Variation of S_{21} with via separation

V_s (mm)	V_s at 5.8 GHz (λ)[a]	S_{21}(Single fence) (dB)	S_{21} (Two fence) (dB)
11	$\lambda/3$	−4.02	−6.26
5.5	$\lambda/6$	−11.96	−19.07
3.67	$\lambda/8$	−18.11	−27
2.75	$\lambda/11$	−22.2	−29.93
2.2	$\lambda/14$	−24.57	−30.45
1.83	$\lambda/16$	−25.78	−30.88
1.57	$\lambda/19$	−26.21	−30.99

[a]Values are approximated integers.

TABLE 3 Variation of S_{21} with via diameter

V_d (mm)	V_d at 5.8GHz (λ)[a]	S_{21} (Single fence) (dB)	S_{21} (Two fence) (dB)
0.2	$\lambda/150$	−14.29	−23.4
0.4	$\lambda/75$	−14.49	−26.62
0.6	$\lambda/50$	−18.77	−28.49
0.8	$\lambda/38$	−21.98	−30.06
1	$\lambda/30$	−24.45	−31.93
1.2	$\lambda/25$	−26.2	−33.25

[a]Values are approximated integers.

and $V_s = 5.5$ mm is obtained at 7.5 and 15.8 GHz. The V_s values, 11 mm and 5.5 mm, are close to $\lambda/2$ as 7.2 and 15.8 GHz, respectively. From this analysis and the data in the tables, a design guideline could be set for via-fences that is for an operating frequency the via separation should be much smaller than $\lambda/2$, anything in range of 5 to 10 times smaller than $\lambda/2$ would be sufficient. On the other hand, for via diameter, anything above $\lambda/30$ would be reasonable. A high-pass filter analogy of via-fence could also explain a lower S_{21} value with two fences. With high-pass filter comparison, the two-fence model is considered as the second-order high-pass filter, whose descending slope rate in band stop region would be twice the slope of single fence and therefore there will be lower S_{21} values.

6 | ARRAY OF SLOT-RING ANTENNA WITH VIA-FENCE

A phased array antenna panel of proposed annular slot-ring patch antenna with via-fence is developed and fabricated. With the application of via-fence, mutual coupling can be in control and would not affect performance in the array development with number of elements.

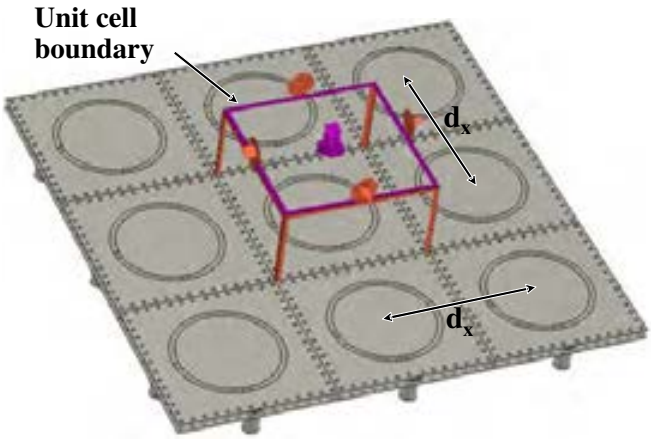

FIGURE 22 Unit element of an array with unit cell boundary and unit cell periodic expansion

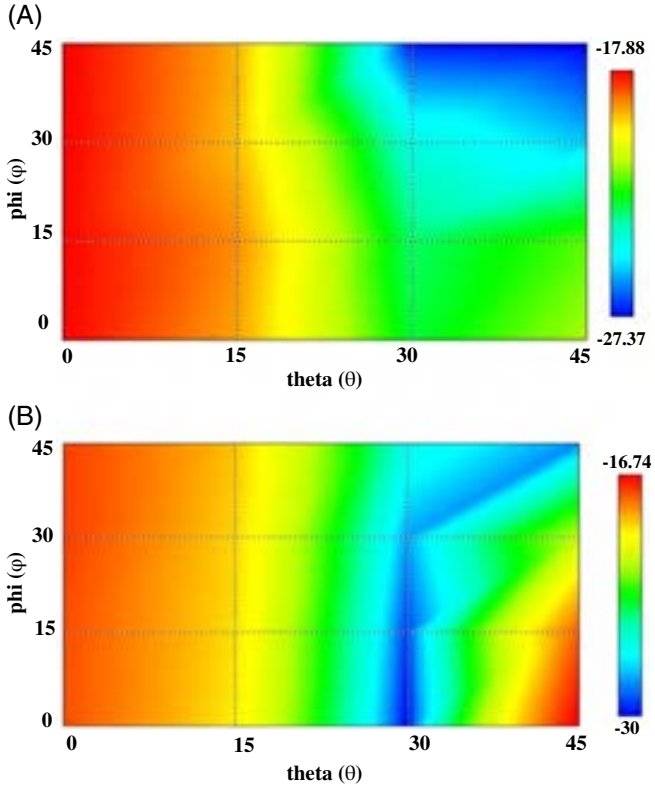

FIGURE 23 Scan impedance at various scan angles (θ, ϕ). A, Port 1. B, Port 2

Via-fence, as verified in previous section, plays a great role isolating the element in array and we observed that gain of the array does not deteriorate much with scanning; however, slot-ring parameters would be required to optimize slightly in order to achieve good matching at 5.8 GHz over the entire scanning range in azimuth and elevation plane. With the simple construction of annular slot-ring antenna, there are only three parameters of the

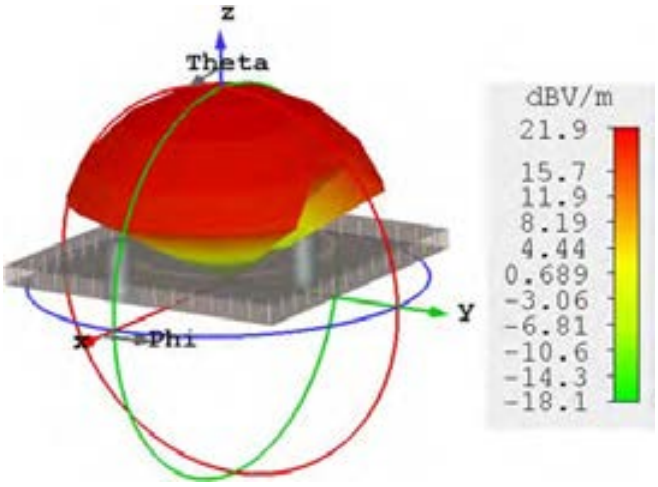

FIGURE 24 Active element pattern over $-60^{\circ} \leq \theta \leq 60^{\circ}$ and $-60^{\circ} \leq \phi \leq 60^{\circ}$

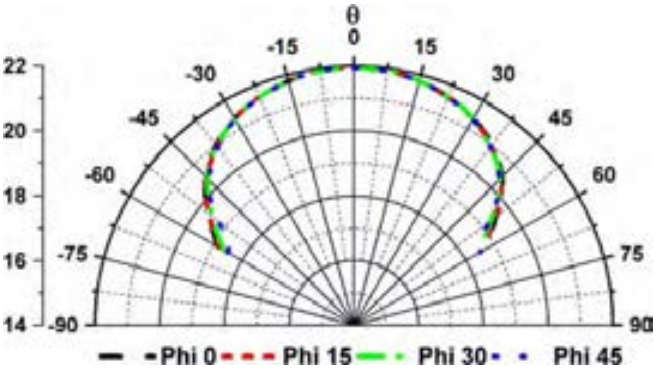

FIGURE 25 Gain of unit cell with scan angles

design, that is, extended feed length (fl_e), inner ring radius (a), and slot width (w_s), that are required to optimize and match the antenna for $\pm 45^{\circ}$ scan angles. The analysis of full 3D phased array antenna computationally would be very exhausting and expensive in terms of system memory usages and time required. The computation of active element pattern is very helpful in large phase array antenna analysis, where only single-element pattern is required to be calculated in the presence of other elements in array with other element ports being terminated.[38,39] Correspondingly, in numerical computation, such as FDTD or FEM, by assuming that the phased array antenna is infinite in extent, the full array analysis can be simplified to a single unit cell using Floquet boundary condition (FBC), saving both system memory and computation time substantially.[40] In Reference 41, a 3×3 array with FBC has been utilized to more accurately analyze infinite phased array antenna by also accounting mutual coupling of centered array element to surrounding elements.

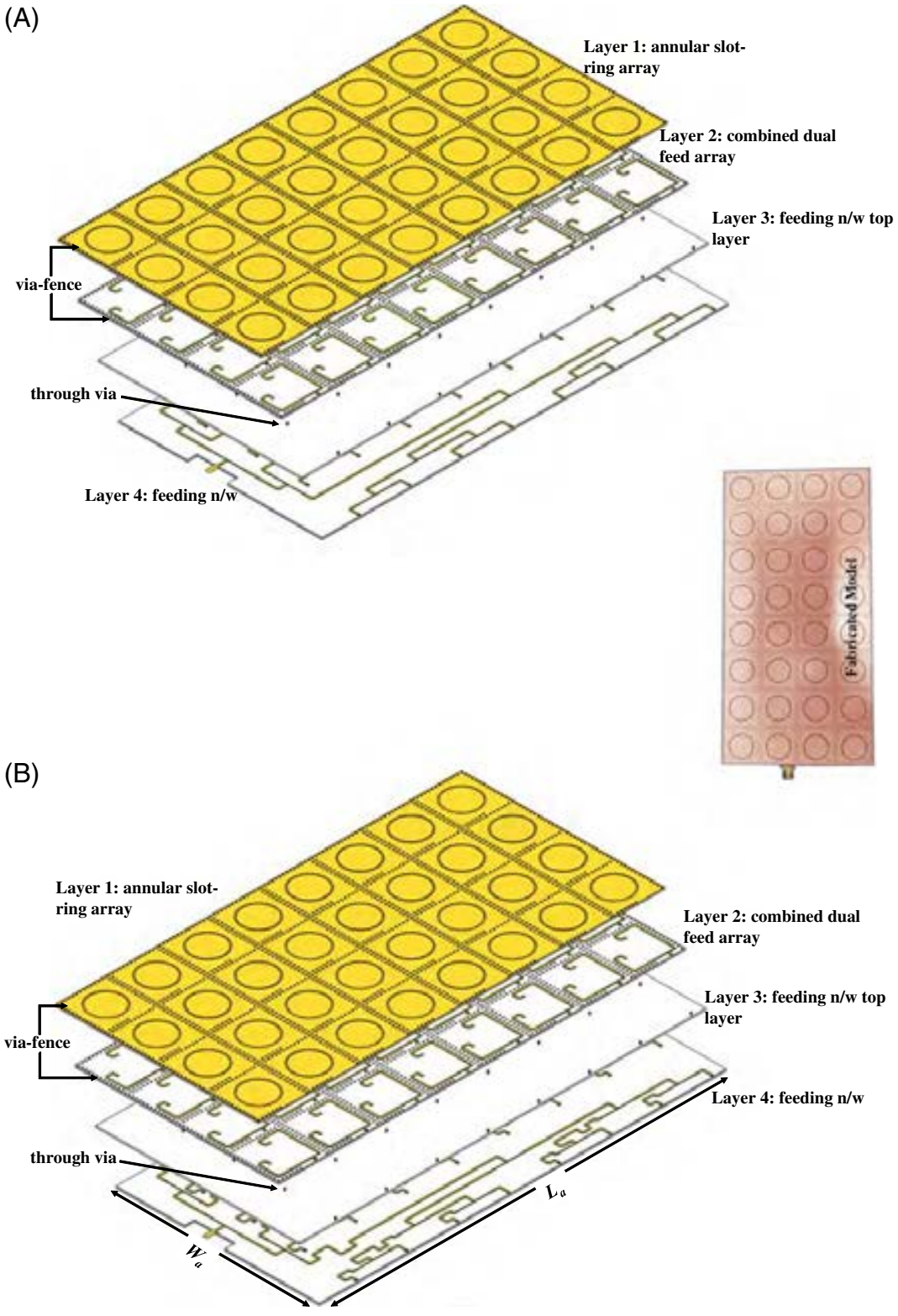

FIGURE 26 4×8 array model for radiation in A, broadside, B, scan angle $\theta = 30^{\circ}$

Recently, CST (commercial software for electromagnetic simulation) has incorporated unit-cell boundary feature in its software to analyze full array and predict scan performance of uniform phased array antenna.[42] We used CST for the development of an array of 4×8 element of annular slot-ring antenna with via-fence. A unit cell boundary applied unit-element of annular slot-ring antenna with its periodic expansion in

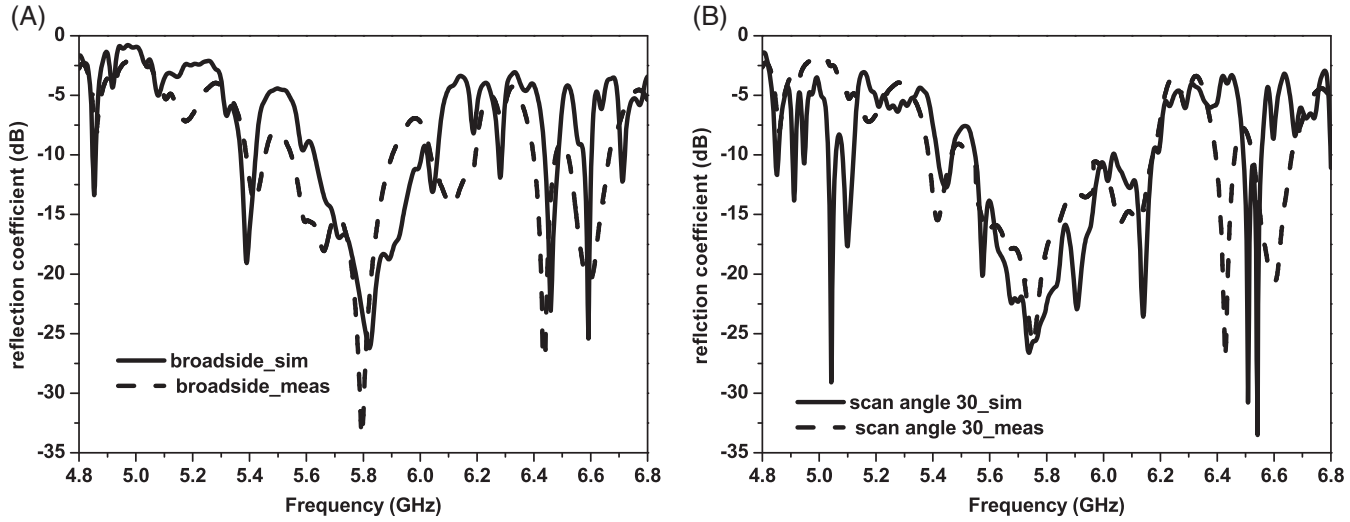

FIGURE 27 4 × 8 array return loss of A, broadside array model, B, scan angle $\theta = 30^{\circ}$ array model

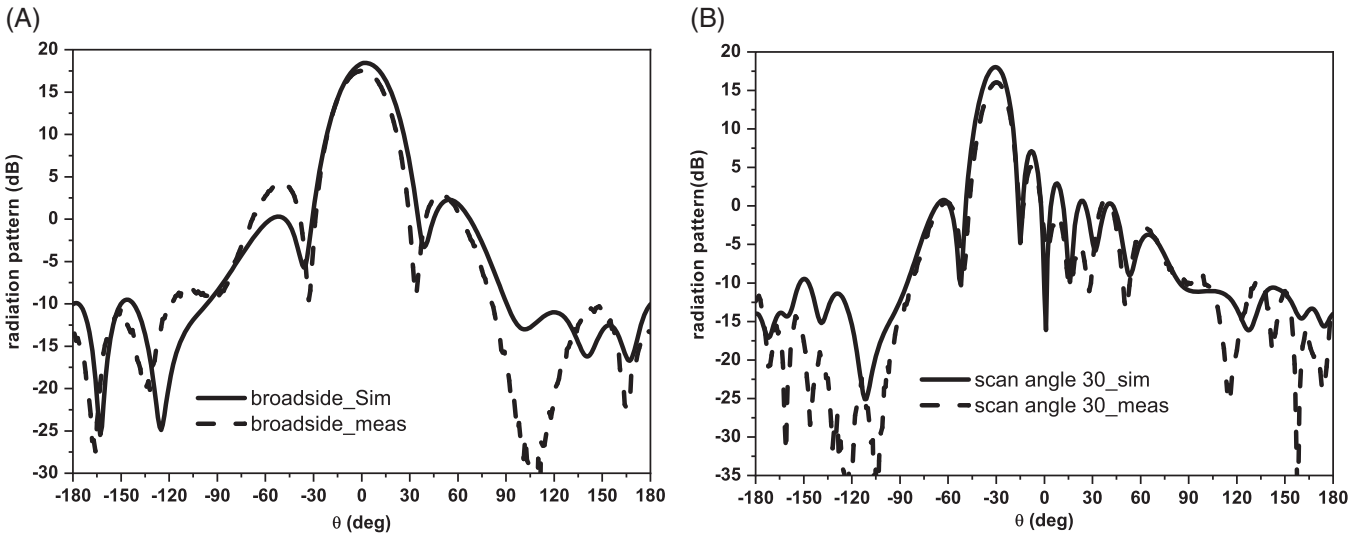

FIGURE 28 4 × 8 array radiation of A, broadside array model, B, scan angle $\theta = 30^{\circ}$ array model

two-dimension is shown in Figure 22. The periodicity of array is d_x (25 mm) in both axes. This model is simulated in CST for various scan angles. Optimization is performed in CST with unit element parameter (a, w_s, fl_e) under unit cell boundary to have an impedance matching over $\pm 45^{\circ}$ in azimuth and elevation plane. The optimized unit-cell scan performance of dual feed port is shown in Figure 23. The active input impedance of the antenna at both feeding ports (Figure 23A,B) is below −15 dB over $\pm 45^{\circ}$ scan in azimuth (ϕ) and elevation angles (θ). Another result is that an active element pattern of antenna element over the scan angle of interest is required to observe and analyze variation in gain with scan angle. Figure 24 is a plot of active element pattern of single element for $-60^{\circ} \leq \theta \leq 60^{\circ}$ and $-60^{\circ} \leq \phi \leq 60^{\circ}$. A two-dimensional (2D) version of Figure 24 is shown in Figure 25, and it is clear from both plots that the drop in gain with scan angle is within 2 dB for $\pm 45^{\circ}$ scanning in elevation and azimuth plane. Such extraordinary results are because of low mutual coupling due to via-fence. The performance of the large array can be predicted from the active element pattern and active impedance characteristics obtained. The active element pattern (Figure 25) multiplied by the AF in Equation (3) provides a good prediction of far-field pattern and scanning performance of large array.

The optimized annular slot-ring antenna is transformed into a 4 × 8 array. The individual port of the

antenna can be fed separately with phase shifter for required beam scanning in MWPT. For the verification of the performance of array formed from the proposed slot-ring element with via-fence, we fabricated two model of the array for radiation in broadside and for scan angle $\theta = 30^{\circ}$. We combined the two feed of annular slot-ring element with a phase shift of 90° using stripline and the entire array of 4×8 element is feed through a stripline corporate feeding network. Two-array model is shown in Figure 26 with fabricated model top view in inset. This is a multilayer model with four layers: layer 1: annular slot-ring array, layer 2: combined dual feed array, and layers 3 and 4: stripline-feeding network. In the two-array model, only the feeding network is different for broadside and scan angle 30° radiation, rest parameters and elements are the same. The feeding network and the combined dual feed lines are connected through vias. The array model manufactured is of $L_a = 200$ mm and $W_a = 100$ mm.

The fabricated array reflection coefficient and radiation pattern is measured and compared with simulated results in Figure 27 and Figure 28. There is a good match in simulated and measured results. The reflection coefficient for the desired frequency of 5.8 GHz is less than 20 dB for broadside and $\theta = 30^{\circ}$ scan angle. The antenna arrays are well matched for different scan angles. The reflection coefficient is better than the predicted S_{11} from unit cell analysis, because in array we added a stripline corporate feeding network circuit with better matching. The gain of the fabricated antenna is 17.7 dB for broadside and 16.2 dB for $\theta = 30^{\circ}$ scan angle. The gain of the array remains within 2 dB as predicted with unit element analysis using Floquet boundary.

7 | CONCLUSION

A concise annular slot-ring microstrip antenna is developed and improvised with the application of via-fence to suit the requirement of planar antenna panel in terms of size and performance for MWPT. Mutual coupling effect in an array is analyzed and diminished using via-fence around each element. Single- and two-row via-fence designs and their effect in restricting surface current flow and therefore reducing the interference among elements in array are analyzed and presented in this article. Closer the vias the better is the isolation between the elements is observed through parametric study. A full array of 4×8 element (100 mm $\times$ 200 mm) is designed using the proposed annular slot-ring antenna with via-fence. FBC is applied to obtain the active element impedance and active element pattern to estimate the full array input impedance and gain with scan angles. A full array for broadside and $\theta = 30^{\circ}$ scan angle with an appropriate feeding network is designed and fabricated. The measured result of the array is similar to the simulated result with good matching at 5.8 GHz of more than 20 dB and gain of 17.7 dB and 16.2 dB at broadside and $\theta = 30^{\circ}$ scan angle, respectively. The annular slot-ring antenna designed is compact in size and has ideal beam scanning characteristics for multipanel retrodirective MPWT system at 5.8 GHz.

ACKNOWLEDGMENTS

This work was supported by the National Research Foundation of Korea (NRF) grant funded by the Korea government (MSIT) (No. 2019R1A2B5B01069407).

ORCID

Laxmikant Minz https://orcid.org/0000-0003-0542-2950

REFERENCES

1. Massa A, Oliveri G, Viani F, Rocca P. Array designs for long-distance wireless power transmission: state-of-the-art and innovative solutions. *Proc IEEE*. 2013;101(6):1464-1481.
2. Shadid R, Noghanian S, Nejadpak A. A literature survey of wireless power transfer. Paper presented at: 2016 IEEE International Conference on Electro Information Technology (EIT); Grand Forks; ND; 2016:0782-0787.
3. Nirmal P, Nandgaonka AB, Nalbalwa SL. A MIMO antenna: study on reducing mutual coupling and improving isolation. Paper presented at: 2016 IEEE International Conference on Recent Trends in Electronics, Information Communication Technology (RTEICT); Bangalore; 2016:173-1740.
4. Shruti D, Snehal L. Mutual coupling reduction techniques in microstrip patch antennas: a survey. *Int Res J Eng Technol*. 2016;03(03):1064-1069.
5. Nadeem I, Choi D. Study on mutual coupling reduction technique for MIMO antennas. *IEEE Access*. 2019;7:563-586.
6. Minz L, Garg R. Reduction of mutual coupling between closely spaced PIFAs. *Electron Lett*. 2010;46(6):392-394.
7. Maddio S, Pelosi G, Righini M, Selleri S, Vecchi I. Mutual coupling reduction in multilayer patch antennas via meander line parasites. *Electron Lett*. 2018;54(15):922-924.
8. Arya AK, Patnaik A, Kartikeyan MV. A compact array with low mutual coupling using defected ground structures. Paper presented at: 2011 IEEE Applied Electromagnetics Conference (AEMC); Kolkata; 2011:1-4.
9. Jolani F, Dadgarpour AM, Dadashzadeh G. Reduction of mutual coupling between dual-element antennas with new PBG techniques. Paper presented at: 2009 13th International Symposium on Antenna Technology and Applied Electromagnetics and the Canadian Radio Science Meeting; Toronto; ON; 2009, 1-4.
10. Mohamadzade B, Afsahi M. Mutual coupling reduction and gain enhancement in patch array antenna using a planar compact electromagnetic bandgap structure. *IET Microw Antenn Propag*. 2017;11(12):1719-1725.
11. Radhi AH, Nilavalan R, Wang Y, Al-Raweshidy H, Eltokhy AA, Aziz NA. Mutual coupling reduction with a novel fractal electromagnetic bandgap structure. *IET Microw Antenn Propag*. 2019;13(2):134-141.

12. Li W, Liu Y, Li Y. Meta-material based mutual coupling reduction of circularly polarized array. Paper presented at: 2016 IEEE International Symposium on Antennas and Propagation (APSURSI); Fajardo; 2016, 511-512.
13. Jiao T, Jiang T, Li Y. A low mutual coupling MIMO antenna using 3-D electromagnetic isolation wall structures. Paper presented at: 2017 Sixth Asia-Pacific Conference on Antennas and Propagation (APCAP); Xi'an; 2017:1-2.
14. Valavan SE, Tran D, Yarovoy AG, Roederer AG. Planar dual-band wide-scan phased array in X-band. *IEEE Trans Antenn Propag*. 2014;62(10):5370-5375.
15. Valavan SE, Tran D, Yarovoy AG, Roederer AG. Dual-band wide-angle scanning planar phased array in X/Ku-bands. *IEEE Trans Antenn Propag*. 2014;62(5):2514-2521.
16. Wang R, Wang B-Z, Hu C, Ding X. Wide-angle scanning planar array with quasi-hemispherical-pattern elements. *Sci Rep*. 2017;7.
17. Wang R, Wang B-Z, Ding X, Ou J-Y. Planar array with bidirectional elements for tunnel environments. *Sci Rep*. 2017;7.
18. Heine C., Beer S., Rusch C., Zwick T. Via-fence antennas on LTCC for radar applications at 122 GHz. Paper presented at: 2013 European Microwave Conference; Nuremberg; 2013: 40-43.
19. El-Halwagy W, Mirzavand R, Melzer J, Hossain M, Mousavi P. A substrate-integrated Fan-beam dipole antenna with varied fence shape for mm-wave 5G wireless. Paper presented at: 2018 IEEE International Symposium on Antennas and Propagation USNC/URSI National Radio Science Meeting; Bostan; MA; 2018:251-252.
20. Yang G, Chen Q, Li J, Zhou S, Xing Z. Improving wide-angle scanning performance of phased array antenna by dielectric sheet. *IEEE Access*. 2019;7:71897-71906.
21. Park H, Kim H. Effective wireless low-power transmission using a phased array antenna. *Microw Opt Technol Lett*. 2015; 57(2):421-424.
22. Lopezf J, Tsay J, Guzman BA, Mayeda J, Lie DYC. Phased arrays in wireless power transfer. Paper presented at: 2017 IEEE 60th International Midwest Symposium on Circuits and Systems (MWSCAS); Boston, MA; 2017:5-8.
23. Malhotra I, Jha KR, Singh G. Beam steering characteristics of highly directive photoconductive dipole phased array antenna for terahertz imaging application. *Opt Quant Electron*. 2019;51(27).
24. Ramesh G, Prakash B, Bahl Inder J, Apisak I. *Microstrip Antenna Design Handbook*. Norwood, MA: Artech House, Inc; 2001.
25. Sim CYD, Lin K-W, Row J-S. Design of an annular-ring microstrip antenna for circular polarization. Paper presented at: IEEE Antennas and Propagation Society Symposium; Monterey; CA; USA; 2004, Vol. 1:471-474.
26. Batchelor JC, Langley RJ. Microstrip annular ring slot antennas for mobile applications. *Electron Lett*. 1996;32(18):1635-1636.
27. Mailloux Robert J. *Phased Array Antenna Handbook*. 3rd ed. Norwood, MA: Artech House, Inc; 2017.
28. Balanis Constantine A. *Antenna Theory: Analysis and Design*. New York, NY: Wiley-Interscience; 2005.
29. Deslandes D, Wu K. Integrated microstrip and rectangular waveguide in planar form. *IEEE Microw Wirel Compon Lett*. 2001;11(2):68-70.
30. Gatti F, Bozzi M, Perregrini L, Wu K, Bosisio RG. A novel substrate integrated coaxial line (SICL) for wide-band applications. Paper presented at: 2006 European Microwave Conference; Manchester; 2006:1614-1617.
31. Suntives A, Khajooeizadeh A, Abhari R. Using via fences for crosstalk reduction in PCB circuits. Paper presented at: 2006 IEEE International Symposium on Electromagnetic Compatibility. 2006 EMC; Portland; OR; USA; 2006, Vol. 1:34-37.
32. Lindseth W. Effectiveness of PCB perimeter via fencing: radially propagating EMC emissions reduction technique. Paper presented at: 2016 IEEE International Symposium on Electromagnetic Compatibility (EMC); Ottawa; ON; 2016:627-632.
33. Farsi S, Aliakbarian H, Schreurs D, Nauwelaers B, Vandenbosch GAE. Mutual coupling reduction between planar antennas by using a simple microstrip U-section. *IEEE Antenn Wireless Propag Lett*. 2012;11:1501-1503.
34. Vishvaksenan KS, Mithra K, Kalaiarasan R, Raj KS. Mutual coupling reduction in microstrip patch antenna arrays using parallel coupled-line resonators. *IEEE Antenn Wireless Propag Lett*. 2017;16:2146-2149.
35. Lee J, Kim S, Jang J. Reduction of mutual coupling in planar multiple antenna by using 1-D EBG and SRR structures. *IEEE Trans Antenn Propag*. 2015;63:4194-4198.
36. Wu G-C, Wang G-M, Liang J-G, Gao X-J, Zhu L. Novel ultra-compact two-dimensional waveguide-based metasurface for electromagnetic coupling reduction of microstrip antenna array. *Int J RF Microw C E*. 2015;25:789-794.
37. Cheng Y, Ding X, Shao W, Wang B. Reduction of mutual coupling Between Patch Antennas Using a Polarization-Conversion Isolator. *IEEE Antenn Wirel Propag Lett*. 2017;16:1257-1260.
38. Pozar D. The active element pattern. *IEEE Trans Antenn Propag*. 1994;42:1176-1178.
39. Pozar DM. A relation between the active input impedance and the active element pattern of a phased array. *IEEE Trans Antenn Propag*. 2003;51:2486-2489.
40. Turner GM, Christodoulou C. FDTD analysis of phased array antennas. *IEEE Trans Antenn Propag*. 1999;47:661-667.
41. Ren J, Gandhi OP, Walker LR, Fraschilla J, Boerman CR. Floquet-based FDTD analysis of two-dimensional phased array antennas. *IEEE Microw Guid Wave Lett*. 1994;4:109-111.
42. Rütschlin M, Wittig T, Iluz Z. Phased antenna array design with CST STUDIO SUITE. Paper presented at: 2016 10th European Conference on Antennas and Propagation (EuCAP); Davos; 2016:1-5.

AUTHOR BIOGRAPHIES

Laxmikant Minz was born in Katihar, India, in September 1986. He received the BTech degree in electronics and communication engineering from NIT Nagpur, India, in 2007 and the MTech, degree in RF and microwave engineering from IIT Kharagpur, India, in 2009. Currently, he is pursuing the PhD degree in the School of Electrical

Engineering, Korea Advanced Institute of Science and Technology (KAIST). His research interests include phased array antenna, mutual coupling reduction, antenna design, and microwave circuit design.

Seong-Ook Park (M'05-SM'11) was born in KyungPook, Korea, in December 1964. He received the BS degree from KyungPook National University, in 1987, the MS degree from Korea Advanced Institute of Science and Technology, Daejeon, in 1989, and the PhD degree from Arizona State University, Tempe, in 1997, all in electrical engineering. From March 1989 to August 1993, he was a Research Engineer with Korea Telecom, Daejeon, working with microwave systems and networks. He later worked in Telecommunication Research Center, Arizona State University, until September 1997. Since October 1997, he has been working as a Professor at the Korea Advanced Institute of Science and Technology. His research interests include mobile handset antenna and analytical and numerical techniques in the area of electromagnetics. Dr Park is a member of Phi Kappa Phi.

How to cite this article: Minz L, Park S-O. Beam scanning annular slot-ring antenna array with via-fence for wireless power transfer. *Int J RF Microw Comput Aided Eng*. 2020;30:e22178. https://doi.org/10.1002/mmce.22178